

PROGRESS IN SRF CH-CAVITIES FOR THE HELIAC CW LINAC AT GSI

M. Miski-Oglu^{1,2*}, K. Aulenbacher^{1,2,3}, W. Barth^{1,2}, M. Basten⁴, C. Burandt^{1,2}, M. Busch⁴,
 T. Conrad⁴, F. Dziuba^{1,2,3}, V. Gettmann^{1,2}, M. Heilmann², T. Kuerzeder^{1,2}, J. List^{1,2,3}, S. Lauber^{1,2,3},
 H. Podlech⁴, A. Rubin², A. Schnase², M. Schwarz⁴, S. Yaramyshev²

¹Helmholtz Institute Mainz, Mainz, Germany

²GSI Helmholtzzentrum für Schwerionenforschung, Darmstadt, Germany

³KPH, Johannes Gutenberg-University, Mainz, Germany

⁴IAP Goethe-Universität Frankfurt, Frankfurt, Germany

Abstract

The machine beam commissioning is a major milestone of the R&D for the superconducting heavy ion continuous wave linear accelerator HELIAC (HELMholtz LInear ACcelerator) of Helmholtz Institute Mainz (HIM) and GSI, developed in collaboration with IAP Goethe-University Frankfurt. During successful beam commissioning of the superconducting 15-gap Crossbar H-mode cavity at GSI Helmholtzzentrum für Schwerionenforschung heavy ions up to the design beam energy have been accelerated. The design acceleration gain of 3.5 MeV has been reached with full transmission for heavy ion beams of up to 1.5 μ A. Fabrication experiences and results of off-line and on-line cavity performance will be presented. The next step is the procurement and commissioning of so called 'Advanced Demonstrator' - the first of series cryomodule for the entire accelerator HELIAC. Results of further Demonstrator beam tests, as well as the status of the Advanced demonstrator project will be reported.

INTRODUCTION

The design and construction of continuous wave (cw) high intensity Linacs is a crucial goal of worldwide accelerator technology development [1]. In the low- and medium-energy range, cw-Linacs can be used for several applications, as for Accelerator Driven subcritical nuclear reactor Systems (ADS) [2, 3] or the synthesis of Super Heavy Elements (SHE) [4] and material science. In particular the increased projectile intensity, preferably in cw mode, would remarkably improve the SHE yield. The compactness and energy efficiency of such cw facilities requires the use of superconducting (sc) elements in modern high intensity ion linacs [5–9]. For this purpose the heavy ion sc cw linac HELIAC is developed at GSI HIM [10, 11] under key support of Institut für Angewandte Physik (IAP) of Goethe University Frankfurt [12, 13].

Table 1 shows the key parameters of the HELIAC. Heavy ion beams with a mass-to-charge ratio up to $A/z = 6$ will be accelerated by twelve multi-gap CH cavities, operated at 216.816 MHz. The HELIAC should serve for physics experiments, smoothly varying the output particle energy from 3.5 to 7.3 MeV/u and simultaneously preserving high beam quality [14].

* m.miskio glu@gsi.de

Table 1: Design Parameters of the HELIAC [13]

| | |
|------------------------------|-----------|
| Mass-to-charge ratio | 6 |
| Frequency (MHz) | 216.816 |
| Max. beam current (mA) | 1 |
| Injection energy (MeV/u) | 1.4 |
| Output energy (MeV/u) | 3.5 – 7.3 |
| Output energy spread (keV/u) | ± 3 |
| SC CH cavities | 12 |

DEVELOPMENT OF CH CAVITIES

360 MHz CH-Cavity Prototype

The superconducting CH-Cavities are the further development of the well established room temperature multi cell H-mode accelerating structures [15] at GSI and IAP. The first milestone in the development of superconducting CH-cavities was the successful design and test of 19-cell prototype cavity with a resonance frequency of 360 MHz, ($\beta_{\text{geom.}} = 0.1$). The prototype cavity has been fabricated

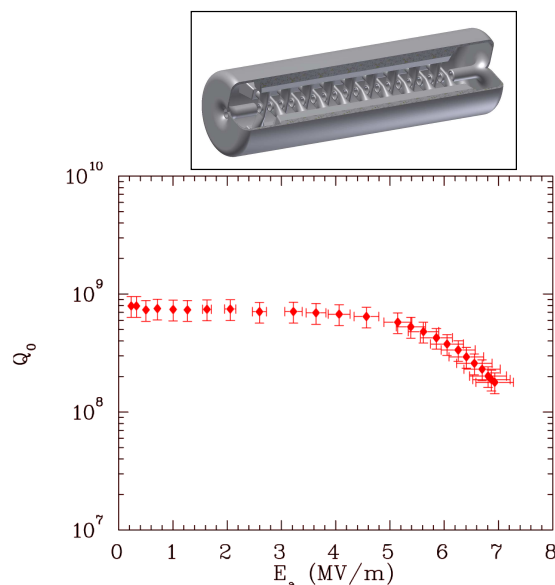


Figure 1: Cross sectional view of CH Prototype (top). Q_0 vs E_a curve for the 360 MHz CH-prototype (bottom) [16].

by Research Instruments (RI) [17] (former ACCEL). The cavity is made from bulk niobium sheets with a thickness of 2 mm and with a RRR value of 250. All parts have been formed either by deep drawing or by spinning. For the cavity production electron beam welding was applied. One special feature of this prototype is the direct welding of the drift tubes into the stems. The length of each drift tube is different (under the conservation of the total cell length) to guarantee a constant field distribution. After the final welding, the cavity has been treated with temperature controlled buffered chemical polishing (BCP) to remove about 120 μm from the surface followed by high pressure rinsing (HPR) using a pressure of about 80 bar. Several cryogenic tests have been performed at IAP since 2005. Before the second surface treatment accelerating gradients of 4.7 MV/m have been achieved [12]. This corresponds to an electric peak field of 25 MV/m. Above peak fields of 20 MV/m strong field emission occurred. The measurement with X-ray TLD-detectors (Thermoluminescence Dosimeter) shows a very strong radiation level close to the cavity center, which indicates a single field emitter. It has been decided to perform an additional Buffered Chemical Polishing (BCP) and High Pressure Rinsing (HPR). After second treatment this resonator reached an accelerating gradient of 7 MV/m (see Fig. 1), this gradient corresponds to total voltage of 5.6 MV [16].

325 MHz CH-Cavity

As a next step a compact, 7-cell, 325 MHz CH-cavity with $\beta_{geom.} = 0.16$ and a tuning system for slow and fast dynamic adjustment of the frequency were designed [18, 19]. The cavity is equipped with two fast tuners of a bellow

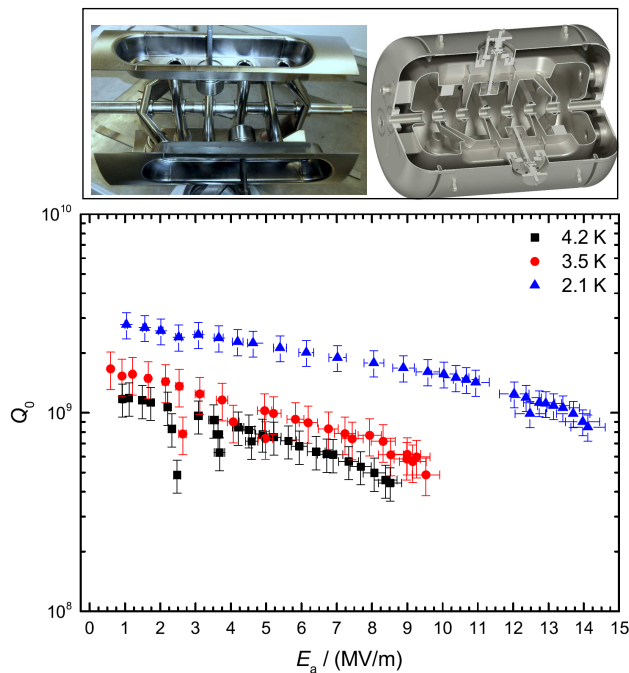


Figure 2: Multigap structure of the 325 MHz CH-cavity during production steps and 3d model of the cavity (top). Measured Q_0 vs E_a curves (bottom) [20].

type geometry which are put inside the cavity. Tuner is connected to the outside by a rod and can be operated by a piezo and a stepping motor drive, respectively. Four additional flanges for surface preparation enable an improved cavity performance after HPR. In order to provide for a compact geometry the inclined stems at the first and last drift tube has been implemented. Inclined end stems yield a more homogeneous field distribution along the beam axis as the magnetic high field volume and correspondingly the inductance is increased. At the same time the longitudinal dimensions of the cavity can be reduced by about 20 % since an extended end cell is not needed for field flattening. After the final welding, the cavity has been treated with BCP (in several steps) to remove about 120 μm from the surface followed by HPR through two beam ports and four of-axis flanges. Consequently, this cavity achieved an accelerating gradient of 8.5 MV/m at 4K resulting in a voltage of 4.2 MV. Furthermore, tests at 2K yielded a gradient of 14.1 MV/m (see Fig. 2) and a voltage of 7 MV, respectively [20].

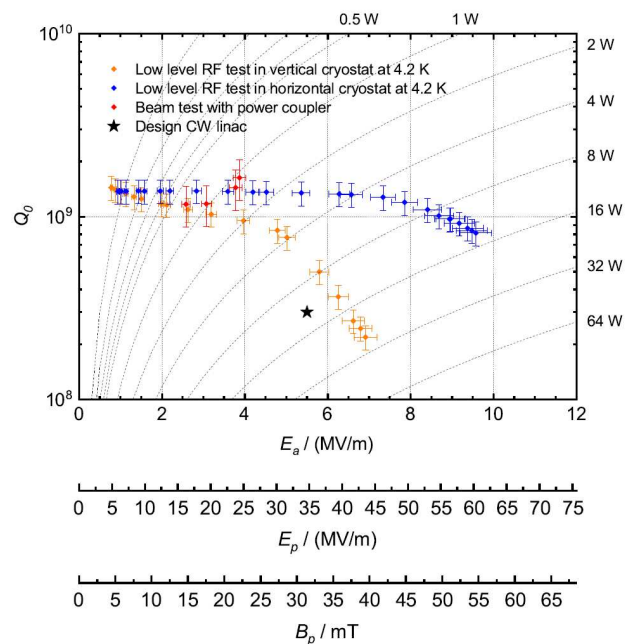


Figure 3: Crosssectional view of 217 MHz CH0 cavity (top). Measured Q_0 vs E_a curve (bottom) [21].

217 MHz Demonstrator Cavity (CH0)

With the promising results from the previous two cavities it was decided to elaborate a newly planned cw heavy ion linac HELIAC based on the CH-type multi-cell resonators.

Content from this work may be used under the terms of the CC BY 3.0 licence (© 2019). Any distribution of this work must maintain attribution to the author(s), title of the work, publisher, and DOI.

As a first step towards HELIAC the 217 MHz CH cavity (CH0) with 15 equidistant accelerating gaps and $\beta_{\text{geom.}} = 0.059$ has been developed [22]. The geometry of CH0 is even more complex and challenging than the structure of the 325 MHz CH-cavity due to the higher number of accelerating gaps, tuners and the lower (thus, providing less space) frequency. After final surface preparation (BCP + HPR) the cavity was delivered to IAP for tests in a vertical cryostat surpassing the demanded design gradient and quality factor despite field emission (see Fig. 3, red circles [21]) [23]. After the final assembly of the helium vessel and further HPR preparation at RI, the cavity was tested again at GSI in a horizontal cryostat. The cavity performance was significantly improved due to an additional HPR treatment. The initial design goals have been exceeded and a maximum accelerating gradient of $E_{\text{acc}} = 9.6 \text{ MV/m}$ at $Q_0 = 8.14 \times 10^8$ has been achieved [21].

CH1/2 for the HELIAC Project

Another step paving the way to HELIAC was realized within the development of the Advanced Demonstrator concept [6, 13]. For this cryomodule scheme two structurally identical CH-cavities with $\beta_{\text{geom.}} = 0.069$ (CH1 and CH2 in the HELIAC pattern) have been developed at IAP [24]. Compared to recent sc CH-cavities both cavities are designed without girders and with stiffening brackets on each inclined end cap (see Fig. 4) aiming for easier manufacturing, increased mechanical stiffness and reduced pressure sensitivity. Each cavity is equipped with two dynamic bellow tuners to adjust the frequency accordingly. After fabrication and surface processing of CH1 this cavity reached a gradient of $E_{\text{acc}} = 9 \text{ MV/m}$ corresponding to 3.32 MV at $Q_0 = 2.4 \times 10^8$ in a first vertical test setup at IAP (see Fig. 4). Recently this cavity has been returned to RI for further surface cleaning processes. The CH2 cavity is just before rf-testing in a vertical cryostat. After the final preparation steps by vendor and assembly of the helium jacket, both cavities would be delivered to GSI for the final acceptance rf-tests.

As a follow up of CH0, CH1 and CH2 the next HELIAC cavities are under design investigation with a special emphasis on peak surface electrical field and tuner design. Figure 5 shows the present simulation status [25].

BEAM TESTS OF DEMONSTRATOR

Prior the realization of HELIAC, the demonstrator project is accomplished at GSI and HIM in collaboration with IAP. The demonstrator setup is located downstream of the GSI High Charge State Injector [26] (HLI).

The demonstrator comprises the 15 gap sc CH-cavity (CH0) [22] embedded by two superconducting solenoids; all three components are mounted on a common support frame (see Fig. 6). The beam focusing solenoids provide a maximum magnetic fields of 9.3 T with a free beam aperture of 30 mm. Each solenoid consists of a main Nb_3Sn -coil and two compensation coils made of NbTi. The compensation

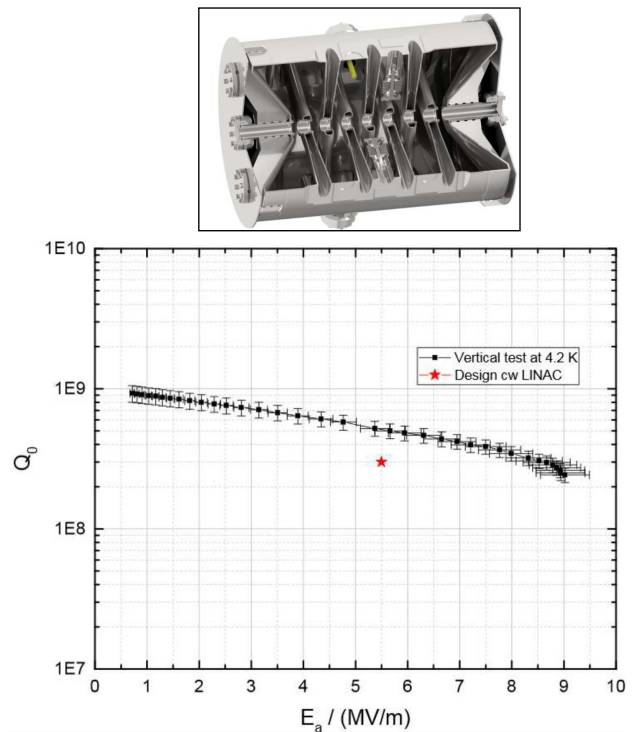


Figure 4: Crosssectional view of CH1/CH2 cavity (top). Measured Q_0 vs E_a curve (bottom) [24].

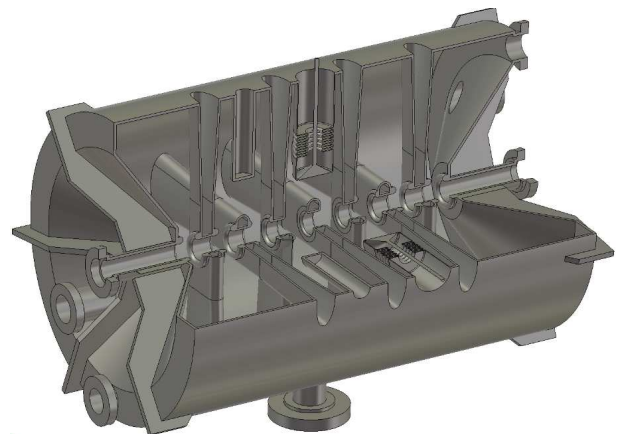


Figure 5: Design status of 216.7 MHz CH3 cavity for the HELIAC project [25].

coils reduce stray field to maximum 30 mT at a longitudinal distance of 300 mm from the center of the main coil. A 3000 liter Helium reservoir in vicinity of the radiation protection shelter is sufficient to provides 2 weeks of cryogenic operation.

Prior to beam commissioning of the cavity, the rf-power couplers were tested and conditioned in a dedicated test resonator [27, 28]. Inside ISO4 class clean room, the power couplers were integrated in the rf-cavity, as well as three frequency tuners, developed at IAP and manufactured at GSI. Furthermore, the CH-cavity and together with solenoids were assembled into a common string. After leak testing the accelerating string was integrated into the cryostat outside

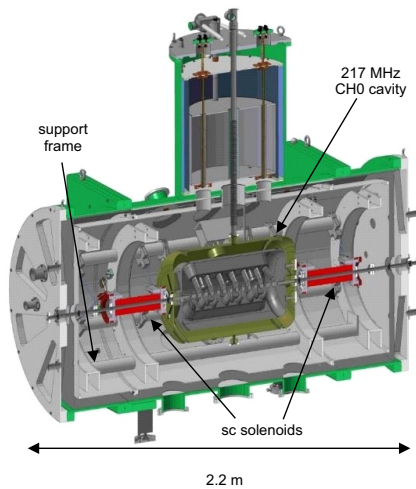


Figure 6: Sectional view of Demonstrator cryostat, the 216.816 MHz CH-cavity and two sc solenoids are suspended within a support frame.

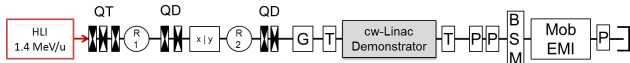


Figure 7: Layout of matching line to the Demonstrator and beam diagnostics test bench. QT/QD=quadrupole triplet/duplet, R = rebuncher, X/Y = beam steerer, G = SEM grid, T = current transformer, P = Phase probe, BSM = bunch shape monitor, EMI = emittance meter.

of the clean room. Figure 7 shows the matching beam line equipped with beam instrumentation devices. It includes beam current transformers, Faraday cups, SEM-profile grids, a dedicated emittance meter, a bunch shape monitor and phase probe pickups (beam energy measurements applying time of flight) provide for proper beam characterization behind the demonstrator.

In June 2017, after a short commissioning of the demonstrator setup and matching line and ramp-up time of some days, the CH0-cavity accelerated for the first time heavy ion beam (Ar^{11+}) with full transmission up to the design beam energy of 1.866 MeV/u ($\Delta W_{\text{kin}} = 0.5 \text{ MeV/u}$). For the first beam test the sc cavity provided an accelerating voltage of more than 1.6 MV. Furthermore, the design acceleration gain of 3.5 MV has been verified and even exceeded by acceleration of Ar^{6+} beam with higher mass to charge ratio $A/z = 6.7$. A maximum average beam intensity of 1.5 μA has been achieved, limited only by the beam intensity of the ion source and maximum duty factor (25 %) of the HLI, while the CH-cavity was operated in cw-mode. All presented measurements were accomplished with high duty factor beam and maximum beam intensity from the HLI. A systematic 2-D scan of beam energy and beam transmission for a wide area of different accelerating fields and rf-phases has been performed. The smooth variation of the beam energy with ramped accelerating gradient could be observed for different rf-phase settings, while the beam trans-

mission was kept above 90 %. Exemplary transversal beam emittance have been measured for accelerated Ar^{9+} beam by a slit grid emittance meter. The measured 90 % emittances in the horizontal and vertical plane are only 0.74 μm and 0.47 μm respectively. The measured (normalized) beam emittance growth at full beam transmission is sufficiently low: 15 % in horizontal plane and 10 % in vertical plane [6]. Besides beam energy measurements the bunch shape was measured with a bunch shape monitor. Impressively small minimum bunch length of about 300 ps (FWHM) and 500 ps (base) could be detected, sufficient for further matching to and acceleration in future rf-cavities

During the beam time in November/December 2018 the result of beam time 2017 were confirmed and further detailed investigation of the longitudinal phase space [29] and further rf-characterization of the CH-cavity [30] were accomplished. Figure 8 shows the measured beam energy (TOF) of the accelerated Ar^{9+} beam as function of the rf-phase for different rf-amplitudes measured at pick-up probe. The measured dissipated power $P_c = P_f - P_r$ in the cavity and quality factor [30] define the stored energy in the cavity. The knowledge of

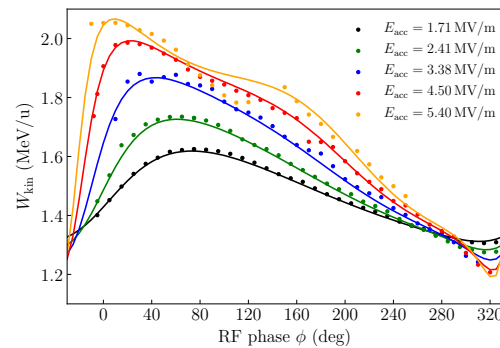


Figure 8: Measured (filled circles) and simulated (solid lines) phase scans for different accelerating gradients.

the stored energy together with the calculated electric field by CST Microwave Studio[®] [31] (normalized to 1 Joule stored energy) allows assignment of the measured pick-up signal to the unique accelerating gradient. The curves in the Fig. 8 show the calculated kinetic energy gain as function of the cavity phase for different accelerating gradients. The curves are obtained by numerical solution of equation of motion for charged particle in the "real" electric field as exported from CST Microwave Studio[®]. The agreement of calculated curves with results of TOF measurements confirm the reliability of rf measurements (*i.e.* quality factor) and calibration of the pick-up probe.

ADVANCED DEMONSTRATOR

Following the successful beam test of the CH0 cavity within the Demonstrator research project, the next milestone is the construction, commissioning and operation of the Advanced Demonstrator cryomodule. It contains the demonstrator CH0 cavity, two identical CH1 & CH2 cavities [24],

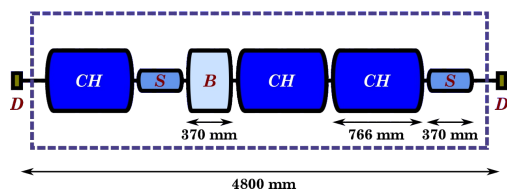


Figure 9: Layout of the Advanced Demonstrator cryomodule containing three CH cavities, a re-buncher cavity (B) and two solenoids (S).

two-gap re-buncher cavity (B) [32, 33] and two sc solenoids (S). Figure 9 shows the layout of the components within the cryomodule. In the future, the Advanced Demonstrator is foreseen to be used as the first of a series of four cryomodules of the HELIAC accelerator. According to beam dynamic simulation [13], the Advanced Demonstrator module will provide for beam energies of up to $W_{kin} = 2.7$ MeV/u for heavy ion beams with $A/z = 6$ and up to $W_{kin} = 3.3$ MeV/u for lighter beams with $A/z = 3$. The two-gap re-buncher cavity is already designed; the procurement of the Nb material has been started.

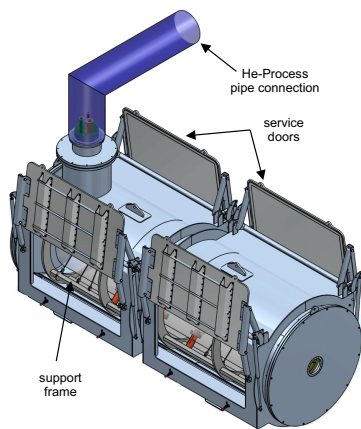


Figure 10: 3-D model of the Advanced Demonstrator cryomodule.

Figure 10 shows the 3-D model of the Advanced Demonstrator cryostat. All components will be cleaned and added to the accelerator string within a ISO4 clean room [34] at HIM. After the vacuum leak test, the string is integrated into the cryostat outside the clean room. The large service doors of the cryostat allow easy assembly of the "cold" and "warm" parts of the power couplers after integration of the accelerator string into the cryostat. Moreover, it allows the *in situ* alignment to the beam axis after installation of the cryomodule in the tunnel for each individual component. The newly build Advanced Demonstrator testing area at GSI provides an enlarged radiation protection shelter, the connection to the cryo plant via dedicated Helium distribution valve box, a new rf gallery equipped with four 3 kW rf-amplifiers and a new control room.

OUTLOOK

In the future the existing UNILAC (UNIversal Linear Accelerator) [35–38] at GSI will be exclusively used as an injector for FAIR to provide short-pulse high-intensity heavy ion beams at low repetition rates [39–42].

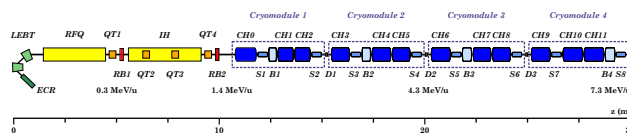


Figure 11: Layout of the HELIAC accelerator.

The new superconducting heavy ion Linac HELIAC (see Fig. 11) should provide ion beams above the Coulomb barrier to ensure the GSI SHE program remains competitive world wide. The Linac design comprises a room temperature cw injector, low energy beam transport (LEBT) section followed by a sc Drift Tube Linac (DTL) consisting of 12 sc CH structures grouped into four cryomodules (CM1-CM4). Besides acceleration of the design ions the HELIAC can be operated with different ions from protons ($A/z = 1$) to U^{28+} ($A/z = 8.5$). From the beam dynamics point of view, an output energy of up to 10 MeV/u for light ions (14 MeV for protons) could be reached without significant performance degradation.

REFERENCES

- [1] C. R. Prior, "Overview of high intensity accelerator projects", in *Proc. 46th ICFA Advanced Beam Dynamics Workshop on High-Intensity and High-Brightness Hadron Beams (HB'10)*, Morschach, Switzerland, Sep.-Oct. 2010, (Morschach, Switzerland), Sep. 2010, pp. 6–10. doi: MOT02.
- [2] Z.-J. Wang *et al.*, "Beam commissioning for a superconducting proton linac", *Phys. Rev. Accel. Beams*, vol. 19, p. 120101, 12 2016. doi: 10.1103/PhysRevAccelBeams.19.120101.
- [3] S. M. Polozov and A. D. Fertman, "High-energy proton beam accelerators for subcritical nuclear reactors", *Atomic Energy*, vol. 113, no. 3, pp. 192–200, 2013. doi: 10.1007/s10512-012-9616-4.
- [4] J. Khuyagbaatar *et al.*, " $^{48}\text{Ca} + ^{249}\text{Bk}$ fusion reaction leading to element $Z = 117$: Long-lived α -decaying ^{270}Db and discovery of ^{266}Lr ", *Phys. Rev. Lett.*, vol. 112, p. 172501, 17 2014. doi: 10.1103/PhysRevLett.112.172501.
- [5] I. Mardor *et al.*, "The Soreq Applied Research Accelerator Facility (SARAF): Overview, research programs and future plans", *EPJ A*, vol. 54, no. 5, p. 91, 2018. doi: 10.1140/epja/i2018-12526-2.
- [6] W. Barth *et al.*, "First heavy ion beam tests with a superconducting multigap ch cavity", *Phys. Rev. Accel. Beams*, vol. 21, p. 020102, 2 2018. doi: 10.1103/PhysRevAccelBeams.21.020102.
- [7] N. Sakamoto *et al.*, "Construction Status of the Superconducting Linac at RIKEN RIBF", in *Proc. 29th Linear Accelerator Conference (LINAC'18)*, Beijing, China, 16-21 September 2018, (Beijing, China), Jan. 2018, pp. 620–625. doi: doi: 10.18429/JACoW-LINAC2018-WE2A03.

- [8] P. Ostroumov *et al.*, “Accelerator Physics Advances in FRIB (Facility for Rare Isotope Beams)”, in *Proc. 9th International Particle Accelerator Conference (IPAC’18)*, Vancouver, BC, Canada, April 29-May 4, 2018, (Vancouver, BC, Canada), Jun. 2018, pp. 2950–2952. doi: doi : 10 . 18429 / JACoW - IPAC2018 - THYGBF4.
- [9] Z. Conway, B. Guilfoyle, H. Guo, M. Kedzie, M. Kelly, and T. Reid, “Progress Toward 2 K High Performance Half-wave Resonators and Cryomodule”, in *Proc. of International Conference on RF Superconductivity (SRF’17)*, Lanzhou, China, July 17-21, 2017, (Lanzhou, China), Jan. 2018, pp. 692–694. doi: <https://doi.org/10.18429/JACoW-SRF2017-WEYA05>.
- [10] W. Barth *et al.*, “Superconducting CH-cavity heavy ion beam testing at GSI”, *J. Phys. Conf. Ser.*, vol. 1067, p. 052007, 2018. doi: 10.1088/1742-6596/1067/5/052007.
- [11] S. Yaramyshev *et al.*, “Advanced approach for beam matching along the multi-cavity SC CW linac at GSI”, *J. Phys. Conf. Ser.*, vol. 1067, p. 052005, 2018. doi: 10.1088/1742-6596/1067/5/052005.
- [12] H. Podlech, U. Ratzinger, H. Klein, C. Commenda, H. Liebermann, and A. Sauer, “Superconducting CH structure”, *Phys. Rev. ST Accel. Beams*, vol. 10, p. 080101, 8 2007. doi: 10.1103/PhysRevSTAB.10.080101.
- [13] M. Schwarz *et al.*, “Beam dynamics simulations for the new superconducting CW heavy ion LINAC at GSI”, *J. Phys. Conf. Ser.*, vol. 1067, p. 052006, 2018. doi: 10.1088/1742-6596/1067/5/052006.
- [14] W. Barth *et al.*, “A superconducting cw-linac for heavy ion acceleration at gsi”, *EPJ Web Conf.*, vol. 138, p. 01026, 2017. doi: 10.1051/epjconf/201713801026.
- [15] U. Ratzinger, “Commissioning of the new gsi high current linac and hif related rf linac aspects”, *Nuclear Instruments and Methods in Physics Research Section A: Accelerators, Spectrometers, Detectors and Associated Equipment*, vol. 464, no. 1, pp. 636–645, 2001. doi: [https://doi.org/10.1016/S0168-9002\(01\)00155-3](https://doi.org/10.1016/S0168-9002(01)00155-3).
- [16] H. Podlech, A. Bechtold, M. Busch, H. Klein H. amd Liebermann, and U. Ratzinger, “Development of the superconducting CH-cavity and applications to proton and ion acceleration”, in *Proc. 13th Int. Conf. RF Superconductivity (SRF’07)*, (Beijing, China), Oct. 2007, p. XX. doi: M0403.
- [17] <https://research-instruments.de>
- [18] M. Amberg *et al.*, “The fast piezo-based frequency tuner for sc ch-cavities”, in *Proceedings of LINAC2014*, Geneva, Switzerland, LINAC, 2014.
- [19] M. Busch *et al.*, “Status of the 325 mhz sc ch-cavity at iap frankfurt”, in *Proc. 2nd Int. Particle Accelerator Conf. (IPAC’11)*, (San Sebastian, Spain), Sep. 2011, pp. 268–270. doi: MOPC083.
- [20] M. Busch, M. Amberg, B. M., F. D. Dziuba, H. Podlech, and U. Ratzinger, “Recent measurements on the sc 325 mhz ch-cavity”, in *Proc. 17th Int. Conf. RF Superconductivity (SRF’15)*, (Whistler, Canada), Sep. 2015, pp. 255–257. doi: MOPB065.
- [21] F. Dziuba *et al.*, “First Cold Tests of the Superconducting cw Demonstrator at GSI”, in *Proc. of Russian Particle Accelerator Conference (RuPAC’16)*, (St. Petersburg, Russia), Nov. 2017, pp. 83–85. doi: doi : 10 . 18429 / JACoW - RuPAC2016 - WECBMH01.
- [22] F. Dziuba *et al.*, “Development of superconducting crossbar-H-mode cavities for proton and ion accelerators”, *Phys. Rev. ST Accel. Beams*, vol. 13, p. 041302, 4 2010. doi: 10.1103/PhysRevSTAB.13.041302.
- [23] F. Dziuba *et al.*, “First Performance Test on the Superconducting 217 MHz CH Cavity at 4.2 K”, in *Proc. of Linear Accelerator Conference (LINAC’16)*, (East Lansing, MI, USA), Sep. 2016, pp. 953–955. doi: <https://doi.org/10.18429/JACoW-LINAC2016-THPLR044>.
- [24] M. Basten *et al.*, “Cryogenic Tests of the Superconducting $\beta = 0.069$ CH-cavities for the HELIAC-project”, in *Proc. 29th Linear Accelerator Conference (LINAC’18)*, Beijing, China, 16-21 September 2018, (Beijing, China), Jan. 2019, pp. 855–858. doi: doi : 10 . 18429 / JACoW - LINAC2018 - THP0072.
- [25] M. Busch *et al.*, “Overview on SC CH-Cavity Development”, in *Proc. 10th International Particle Accelerator Conference (IPAC’19)*, (Melbourne, Australia), May 2019, pp. 2822–2825. doi: doi : 10 . 18429 / JACoW - IPAC2019 - WEPB012.
- [26] P. Gerhard *et al.*, “Commissioning of a new cw radio frequency quadrupole at GSI”, in *Proc. 1st Int. Particle Accelerator Conf. (IPAC’10)*, (Kyoto, Japan), May 2010. doi: MOPD028.
- [27] M. Busch *et al.*, “Update on the SC 325 MHz CH-Cavity and Power Coupler Processing”, in *Proc. of Linear Accelerator Conference (LINAC’16)*, (East Lansing, MI, USA), Sep. 2016, pp. 913–915. doi: <https://doi.org/10.18429/JACoW-LINAC2016-THPLR029>.
- [28] J. List *et al.*, “High Power Coupler R&D for Superconducting CH-cavities”, in *Proc. 29th Linear Accelerator Conference (LINAC’18)*, Beijing, China, 16-21 September 2018, (Beijing, China), Jan. 2019, pp. 920–923. doi: doi : 10 . 18429 / JACoW - LINAC2018 - THP0107.
- [29] S. Lauber *et al.*, “Reconstruction of the longitudinal phase portrait for the sc cw heavy ion heliac at gsi”, in *presented at the 10th International Particle Accelerator Conf. (IPAC’19)*, Melbourne, Australia, May 2019, 2019.
- [30] F. Dziuba *et al.*, “Further rf measurements on the superconducting 217 mhz ch demonstrator cavity for a cw linac at gsi”, in *presented at the 10th International Particle Accelerator Conf. (IPAC’19)*, Melbourne, Australia, May 2019, 2019.
- [31] C.-C. S. Technology. www.cst.com
- [32] M. Gusarova, W. A. Barth, S. Yaramyshev, M. Miski-Oglu, M. Basten, and M. Busch, “Design of the two-gap superconducting re-buncher”, *J. Phys. Conf. Ser.*, vol. 1067, p. 082005, 2018. doi: 10.1088/1742-6596/1067/8/082005.
- [33] K. Taletskiy *et al.*, “Comparative study of low beta multi-gap superconducting bunchers”, *J. Phys. Conf. Ser.*, vol. 1067, p. 082006, 2018. doi: 10.1088/1742-6596/1067/8/082006.
- [34] T. Kuerzeder *et al.*, “Cleanroom installations for srf cavities at the helmholtz institute mainz”, in *presented at the 10th International Particle Accelerator Conf. (IPAC’19)*, Melbourne, Australia, May 2019, 2019.
- [35] W. Barth *et al.*, “ U^{28+} -intensity record applying a H_2 -gas stripper cell”, *Phys. Rev. ST Accel. Beams*, vol. 18, p. 040101, 4 2015. doi: 10.1103/PhysRevSTAB.18.040101.
- [36] A. A. Adonin and R. Hollinger, “Beam brilliance investigation of high current ion beams at gsi heavy ion accelerator facility”, *Review of Scientific Instruments*, vol. 85, no. 2, 02A727, 2014. doi: 10.1063/1.4833931. <https://doi.org/10.1063/1.4833931>.
- [37] S. Yaramyshev, W. Barth, L. Groening, A. Kolomiets, and T. Tretyakova, “Development of the versatile multi-particle

code DYNAMION”, *Nuclear Instruments and Methods in Physics Research Section A: Accelerators, Spectrometers, Detectors and Associated Equipment*, vol. 558, no. 1, pp. 90–94, 2006. doi: <https://doi.org/10.1016/j.nima.2005.11.018>.

- [38] W. Barth, W. Bayer, L. Dahl, L. Groening, S. Richter, and S. Yaramyshev, “Upgrade program of the high current heavy ion unilac as an injector for fair”, *Nuclear Instruments and Methods in Physics Research Section A: Accelerators, Spectrometers, Detectors and Associated Equipment*, vol. 577, no. 1, pp. 211–214, 2007. doi: <https://doi.org/10.1016/j.nima.2007.02.054>.
- [39] W. Barth *et al.*, “High brilliance uranium beams for the gsi fair”, *Phys. Rev. Accel. Beams*, vol. 20, p. 050 101, 5 2017.

doi: 10.1103/PhysRevAccelBeams.20.050101.

- [40] W. Barth *et al.*, “Heavy ion linac as a high current proton beam injector”, *Phys. Rev. ST Accel. Beams*, vol. 18, p. 050 102, 5 2015. doi: 10.1103/PhysRevSTAB.18.050102.
- [41] L. Groening *et al.*, “Benchmarking of measurement and simulation of transverse rms-emittance growth”, *Phys. Rev. ST Accel. Beams*, vol. 11, p. 094 201, 9 2008. doi: 10.1103/PhysRevSTAB.11.094201.
- [42] S. Yaramyshev *et al.*, “Virtual charge state separator as an advanced tool coupling measurements and simulations”, *Phys. Rev. ST Accel. Beams*, vol. 18, p. 050 103, 5 2015. doi: 10.1103/PhysRevSTAB.18.050103.